 Hydrology Research | 43.4 | 2012

Up-scaling surface runoff from plot to catchment scale

A. Alaoui, P. Spiess, M. Beyeler and R. Weingartner

ABSTRACT

The main aims of this study were to identify and characterize the flow processes at the plot scale, and to up-scale these processes at the catchment scale by Terrain Analysis, using Digital Elevation Models (TauDEMs) based on *in-situ* sprinkling experiments. To calibrate the TauDEM-based method at the plot scale, *in-situ* sprinkling experiments were carried out on two plot scales (16 m^2 divided into 16 plots of 1 m^2 on various slopes). The marked differences in the textural and structural porosities between forest and grassland soil appear to control runoff processes. While grassland soils were characterized by a variable subsurface flow depending mainly on field slope, deep percolation was mainly found in forest soils. In addition, the map of flow directions also shows that two factors play an important role: on the one hand, the spatial sequence of the areas with a predisposition to surface runoff, and on the other, the tortuosity and length of channels that enhance the cumulative water volume in the target outlets. When based on sprinkling experiments, the TauDEM-based method provides more quantitative information on the dynamic of flow at the catchment scale. Furthermore, additional investigations are needed to validate the calculations of flow at a larger scale.

Key words | digital elevation model, runoff processes, soil hydrology, up-scaling of runoff processes

A. Alaoui (corresponding author)
P. Spiess
M. Beyeler
R. Weingartner
Hydrology Group,
Department of Geography,
University of Bern,
Hallerstrasse 12,
3012 Bern,
Switzerland
E-mail: *alaoui@giub.unibe.ch*

INTRODUCTION

At plot and hillslope scale, many different aspects of runoff formation have been studied in recent years (e.g. Anderson & Burt 1990; Buttle & McDonald 2002; McDonnell 2003; Scherrer *et al.* 2007). To integrate this process knowledge in rainfall-runoff models, information is needed to define the spatial distribution of the runoff processes in the catchment under consideration. For this purpose, methods based on soil data, geology, topography and vegetation for process identification have been developed to delineate dominant runoff processes or zones of predisposition to produce runoff at plot scale (e.g. Peschke *et al.* 1999; Scherrer & Naef 2003; Markart *et al.* 2004). Similarly, Maréchal & Holman (2004) used the Hydrology of Soil Type (HOST) system (Boorman *et al.* 1995) to provide a conceptual representation of the hydrological processes in UK soils. Their model defines the hydrological behaviour of soils in terms of their influence on river flow at the catchment scale and gives a classification of all the soil types of the United Kingdom into 29 conceptual response models (or classes). Based on a similar method, and with the help of sprinkling experiments, Schmocker-Fackel *et al.* (2007) produced maps of the dominant runoff processes that show the potential of each area to produce a given runoff process but fail to establish the hydrologic connectivity between them.

In catchment hydrology, it has been shown that for runoff generation processes, the use of measured *in-situ* parameters cannot be expected to produce accurate predictions at all scales because of the non-linearity of the processes involved, together with the heterogeneity of the natural system (Beven 1995). One way to overcome this is to investigate the channels into which the flow converges and that are characterized by a structured correlation due to a smoothing effect by using, for example, Terrain analysis with Digital Elevation Models (TauDEMs) (Tarboton 1997). The specific catchment area contributing to flow at any particular location is useful for determining relative saturation and

doi: 10.2166/nh.2012.057

runoff generation from saturation excess in models such as Topmodel (Beven & Kirkby 1979; Beven *et al.* 1984; Wood *et al.* 1990).

TauDEMs are appropriate methods to generate high resolution maps of a flow network. Digital data generated by this approach also have the advantage that they can be readily imported and analyzed by Geographic Information Systems (GISs). The technological advances provided by GIS and the increasing availability and quality of Digital Elevation Models (DEMs) have greatly expanded the potential application of TauDEMs to many hydrologic, hydraulic, water resource and environmental investigations (Moore *et al.* 1991). The continuity of the DEM is an important contributor to interpolated gradient values, potentially affecting energy estimates as well as flow directions (Tarboton 1997).

The main aims of this study were: (i) to identify and characterize the flow processes at the plot scale, and (ii) to up-scale these flow processes at the catchment scale, by combining maps of flow directions according to Tarboton (1997), maps of zones of predisposition to surface runoff and *in-situ* sprinkling experiments. The question is how much information is given by such a combination of methods compared with considering the same methods separately?

MATERIAL AND METHODS

Site description

The experiments were carried out during summer 2008 (April–October) at the experimental area called Innerrüteni/Hälfis in Kandergrund (Figure 1) located 1,110 m above sea level (masl) at the east side of the Kander Valley, which spreads out in the north-south direction in the Bernese Oberland in Switzerland (Furrer *et al.* 1993). On the west side of the investigated area, the Kander River is located at 793 masl and can have streamflow discharge as high as 7.7 $m^3 s^{-1}$, as observed during the period between 1961 and 1980 (Schädler & Weingartner 1992). On the eastern part of the investigated area, the glacier deposit of the Kandergrund is divided into two main compartments (Furrer *et al.* 1993): a moraine till deposit at the west side and slope debris on the east side (Table 1 and Figure 1). The mean annual temperature is 5.9 °C and the total annual precipitation is 1,274 mm. In addition to grassland soil (G1–G7), two types of forest were considered in this study: Fa (Fa1, Fa2 and Fa3) and Fb (Fb1, Fb2 and Fb3) corresponding to Spruce forest (*Calamagrostio variae-Pieceetum*) and Fir-Beech forest (*Adenostylo alliariae-Abieti-Fagetum*), respectively. The soil is described as Dystric Cambisol (WRB/FAO) in the grassland and in forest soil Fb, and as Rendzic Leptosol (WRB) (Rendzina (FAO)) in forest soil Fa (USDA, Soil Survey Staff 2003) (Table 1). Its texture consists of clay loam to a depth of 0.60 m in grassland and silt loam in forest soil to a depth of 0.75 m. Its organic carbon content varies from 9 to 9.6% in grassland and from 8.3 to 12.5% in forest soil. A pH varying from 5 to 8 was measured in topsoil and subsoil, respectively, in both grassland and forest soils (Table 2). At both locations, the soil is relatively shallow and the weathered bedrock starts at depths below about 0.30 m.

A total of 19 plots were chosen to carry out the sprinkling experiments (Table 1): six plots of 1 m^2 (G2–G7) and one of 16 m^2 (G1) in grassland, and six plots of 1 m^2 (Fa1-Fa3, Fb1-Fb3) in forest soil. In addition, within G1 (16 m^2) six plots of 1 m^2 (B3, C1, C2, D1-D3) were chosen to conduct the same irrigations with same intensities described above. These plots were chosen because they have different slopes. The aim of such experiments was to calibrate and validate the TauDEM-based method (Tarboton 1997) at the plot scale.

Laboratory analysis

The texture of samples (one sample per depth) was determined after H_2O_2 treatment to remove organic material (Konen *et al.* 2002). The sand fraction of diameter 2000-60 μm was obtained by wet sieving. The amounts of silt (2 < diameter < 60 μm) and clay (diameter < 2 μm) fractions were measured on pre-treated samples by sedimentation with a SediGraph 5100 (Micromeritics, Norcross, USA). The SediGraph 5100 system uses particle sedimentation rates in combination with X-ray absorption. Soil pH was measured 1:2 (soil: 0.01 M $CaCl_2$) on a mass basis (Soil Survey Staff 2004). Organic carbon content was determined by the mass loss on ignition. The same sample was used for the analysis of pH and organic carbon content.

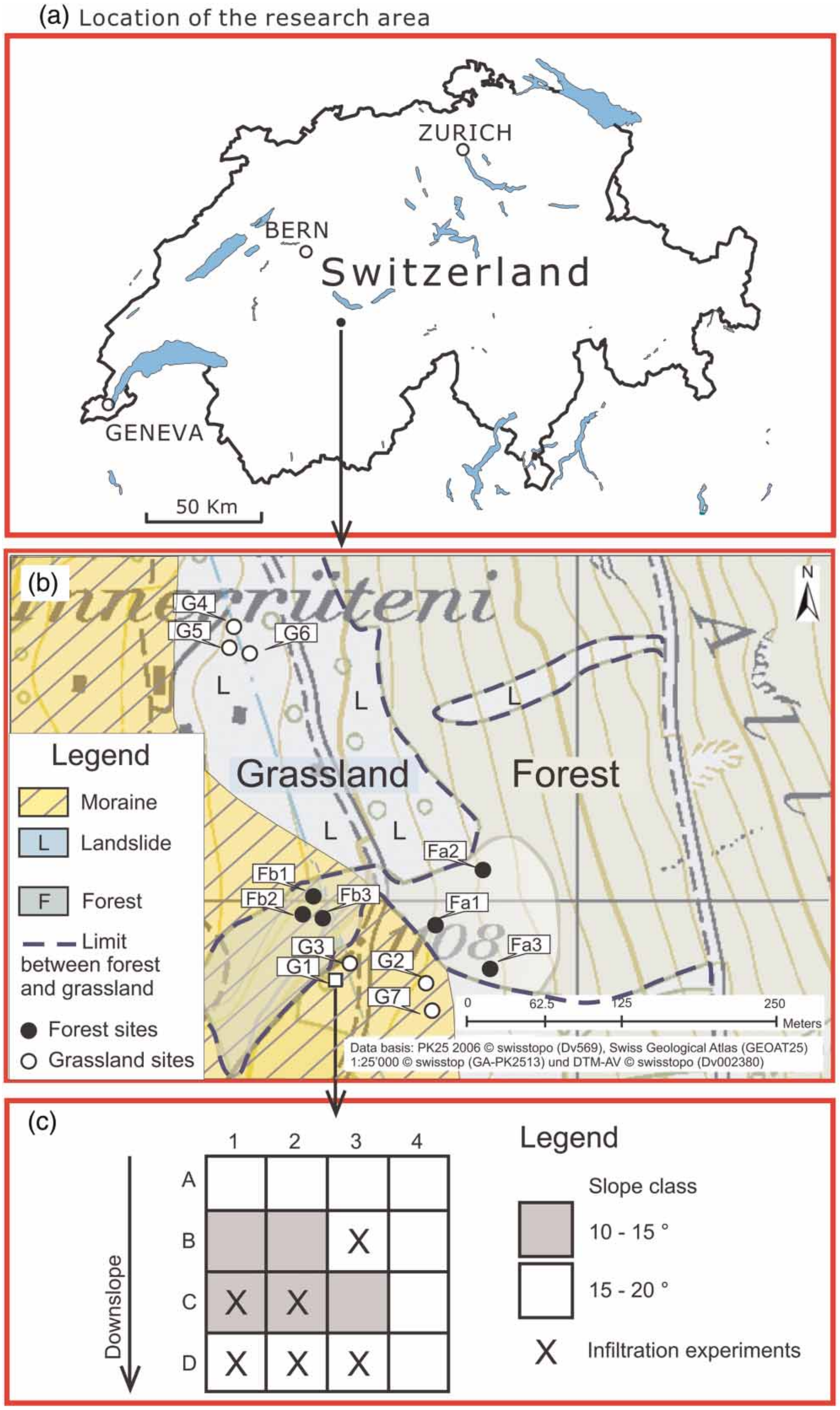

Figure 1 | Location of the catchment under consideration (Innerrüteni, Kandergrund); (a) map of Switzerland with the location of the plots; (b) precise location of the forest (Fa1–Fa3 and Fb1–Fb3) and grassland plots (G1–G7) and (c) location of the small plots of 1 m^2 within G1 (16 m^2).

Table 1 | General characterization of the investigated plots

Hillslopes		Surface [m^2]	Slope [°]	Depth (m) of TDR probes	Vegetation	Geology	Soil type
G1	B3	1	14.8	0.07/0.17/0.45	Grassland	Moraine till deposit (Glacier deposit)	Dystric Cambisol (FAO) (Stones at <0.30 m)
	C1	1	17.6	0.07/0.17/0.45			
	C2	1	18.8	0.07/0.17/0.45			
	D1	1	13.5	0.07/0.17/0.45			
	D2	1	10.6	0.07/0.17/0.45			
	D3	1	12.2	0.07/0.17/0.45			
G1		16	14.7	0.07/0.17/0.45			
G2		1	26.5	0.07/0.17/0.45			
G3		1	5.0	0.07/0.17/0.45			
G7		1	18.0	0.07/0.17/0.45			
Fa1		1	16.6	0.10/0.25/0.50	Spruce forest *(Calamagrostio variae-Pieceetum)*	Slope debris	Rendzina (FAO) (Stones at <0.30 m)
Fa2		1	24.2	0.10/0.25/0.50			
Fa3		1	30.1	0.10/0.25/0.50			
Fb1		1	17.2	0.12/0.27/0.52/0.72	Firs-Beech forest *(Adenostylo alliariae-Abieti-Fagetum)*	Moraine till deposit (Glacier deposit)	Dystric Cambisol (FAO)
Fb2		1	24.3	0.12/0.27/0.52/0.72			
Fb3		1	31.3	0.12/0.27/0.52/0.72			
G4		1	18.0	0.05/0.15/0.30	Grassland	Slope debris	Dysric Cambisol (FAO)
G5		1	25.0	0.05/0.15/0.30			
G6		1	8.0	0.05/0.15/0.30			

For the analysis of total porosity and pore size distribution (PSD), five undisturbed soil samples of 100 cm^3 volume were taken from each soil horizon and three horizons were considered (0.05–0.15, 0.35–0.45 and 0.55–0.65 m soil depths). Total porosity was then determined directly for each undisturbed sample after drying at 105 °C for 24 h assuming a particle density of 2.65 g cm^{-3}. An aggregate of soil was then carefully taken from the dried, undisturbed sample that was selected to avoid desiccation cracks, root pores or other discontinuities. The PSD of this aggregate was analyzed by mercury porosimetry (Fiès 1992). Considered as a non-wetting liquid, the mercury was forced into the dry aggregate by air pressure. The relationship between the equivalent pore diameter (D, in μm) and the applied pressure (P, in kPa) was obtained according to the Jurin–Laplace equation (Fiès 1992). The pressures P used in this operation varied between 4 and 2,000 kPa corresponding to a PSD varying from 360 to 0.006 μm. Three clods of about 2 cm^3 in volume from each soil layer (0.15 and 0.25 m depths) were sampled and oven-dried at 105 °C for 24 h prior to measuring. During the analysis, no shrinkage was observed. The pore classes are defined as follows: (i) micropores are the pores smaller than 0.2 μm equivalent diameter, (ii) mesopores are between 0.2 and 50 μm in diameter, and (iii) macropores are defined to be larger than 50 μm (Sekera 1951; Luxmoore 1981).

In-situ field irrigation experiments

On the 1 m^2 plots, irrigation was supplied by a rainfall simulator: a metallic disc with a surface of 1 m^2 which is perforated with 100 holes attached to small tubes that lead into a reservoir. Irrigation was applied from a height of 0.50 m from the ground. The metallic disc is moved by an electric motor, and the irrigation intensity is controlled by a flow meter (Alaoui & Helbling 2006). Irrigation on the 16 m^2 plot was conducted using a watering can adjusted to uniformly irrigate the entire area; in addition a plastic tarpaulin was fixed around it to prevent any overflowing. The duration of each irrigation was 1 h. The intensities of irrigation were 24, 36 and 48 mm h^{-1}. In this area, the 100-year return period of rainfall is 60 mm h^{-1}.

Table 2 | Basic soil parameters of soil in Kandergrund Valley

Plot	Depth (m)	Particle size distribution (%) Sand (>60 μm)	Silt (2–60 μm)	Clay (<2 μm)	Texture	Organic Carbon OC (%)	pH
Texture, organic carbon and pH of investigated soils in grassland and forest hillslopes							
Fa1	0.10–0.15	37.2	52.6	10.2	Silt loam	n.a.	6.0
	0.25–0.30	35.5	56.1	8.4	Silt loam	n.a.	6.0
	0.50–0.55	31.9	48.6	19.5	Loam	n.a.	6.5
	0.70–0.75	34.3	46.5	19.2	Loam	n.a.	7.0
Fa2	0.10–0.15	n.a.	n.a.	n.a.	n.a.	n.a.	n.a.
	0.25–0.30	32.1	49.6	18.3	Loam	n.a.	8.0
	0.50–0.55	n.a.	n.a.	n.a.	n.a.	n.a.	n.a.
	0.70–0.75	29.8	56.1	14.1	Silt loam	n.a.	8.0
Fa3	0.10–0.15	27.9	52.7	19.4	Silt loam	n.a.	7.0
	0.25–0.30	29.6	50.0	20.4	Silt loam	n.a.	8.0
	0.50–0.55	30.9	49.2	19.9	Loam	n.a.	8.0
	0.70–0.75	34.9	41.3	23.8	Loam	n.a.	8.0
Fb1	0.10–0.15	20.0	62.9	17.1	Silt loam	12.53	5.5
	0.25–0.30	16.4	61.6	22.0	Silt loam	n.a.	5.5
	0.50–0.55	14.2	51.9	33.9	Silty clay loam	10.03	8.0
	0.70–0.75	20.5	46.7	32.8	Clay loam	8.27	8.0
Fb2	0.10–0.15	23.2	61.1	15.7	Silt loam	6.57	6.0
	0.25–0.30	30.5	56.4	13.1	Silt loam	n.a.	7.0
	0.50–0.55	25.0	51.6	23.4	Silt loam	7.14	8.0
	0.70–0.75	23.0	44.2	32.8	Clay loam	7.66	8.0
Fb3	0.10–0.15	17.5	54.4	28.1	Silty clay loam	12.73	5.5
	0.25–0.30	13.0	46.2	40.8	Silty clay	n.a.	8.0
	0.50–0.55	21.1	36.9	42.0	Clay	10.46	8.0
	0.70–0.75	17.3	43.4	39.3	Silty clay loam	9.93	8.0
G1(B3)/G2	0.05–0.10	28.2	45.1	26.7	Clay loam	n.a.	5.5
	0.15–0.20	27.9	41.4	30.7	Clay loam	8.90	5.5
	0.25–0.30	28.9	41.8	29.4	Clay loam	n.a.	5.0
	0.35–0.40	38.2	36.2	25.6	Clay loam	9.57	7.5
	0.45–0.50	36.5	39.7	23.8	Loam	n.a.	n.a.
	0.55–0.60	35.0	32.4	32.6	Clay loam	n.a.	n.a.
G3	0.05–0.25	24.1	42.1	33.8	Clay loam	n.a.	5.5
	0.25–0.35	25.2	41.2	33.6	Clay loam	7.97	5.5
	0.35–0.45	25.6	46.9	27.5	Clay loam	9.61	6.0
	0.45–0.55	22.6	42.3	35.1	Clay loam	8.51	5.5
G4	0.05–0.10	19.4	55.7	24.9	Silt loam	7.50	6.0
	0.15–0.25	19.6	52.4	30.0	Silty clay loam	6.30	5.5
	0.25–0.35	24.1	42.0	33.9	Clay loam	6.00	6.5
	0.45–0.55	21.0	35.6	43.4	Clay	n.a.	5.5
G5	0.30–0.35	25.7	43.3	31.0	Clay loam	6.5	5.5

Textural classification was according to the USDA soil taxonomy; n.a.: not available.
Data for G6 and G7 are not available.

Soil moisture was measured using Time Domain Reflectometry (CR10X & TDR100, Campbell Scientific Inc.), with 0.20 m wave guides (two parallel rods of 6 mm diameter). The calibration was performed according to Roth *et al.* (1990) who separated the impact of the wave-guide geometry from the soil properties, such as bulk density and the contents of clay and organic matter, on the dielectric constant. TDR probes were inserted horizontally at four soil depths (0.12, 0.27, 0.52 and 0.72 m) in forest plots (Fa and Fb), at three soil depths in the three grassland plots (0.07, 0.17 and 0.40 m for G1 and G2, and 0.15, 0.25 and 0.35 m for G3 and G4) and at one soil depth (0.15 m) in G5, G6 and G7. TDR data were recorded every 60 s.

Surface runoff out of each plot of 1 m^2 surface area was measured during the irrigation, using a metallic sheet (1×0.50 m) inserted in a soil profile at 0.05–0.10 m depth to collect surface runoff along a width of 1 m. The volume of collected water was measured with a flowmeter (Alaoui *et al.* 2003) and stored automatically in a datalogger (CR10X, Campbell Scientific Inc.). For the 16 m^2 plot, surface runoff was measured with a metallic sheet (4×0.50 m) inserted in a soil profile at 0.5–0.10 m depth to collect surface runoff along a width of 4 m with the same collector described above. In this study, runoff coefficient (RC) specific to an individual rainstorm (i.e. irrigation) is defined as surface runoff divided by the corresponding rainfall, both expressed as depth over plot area (mm).

Principle of the extrapolation of runoff process

To up-scale the runoff process, different main steps are taken into account (Figure 2):

(i) Sprinkling experiments of three different intensities were carried out on each plot of a given slope to attribute a specific value of runoff to a class category.
(ii) Maps of predisposition to surface runoff are delineated using the classification of Markart *et al.*

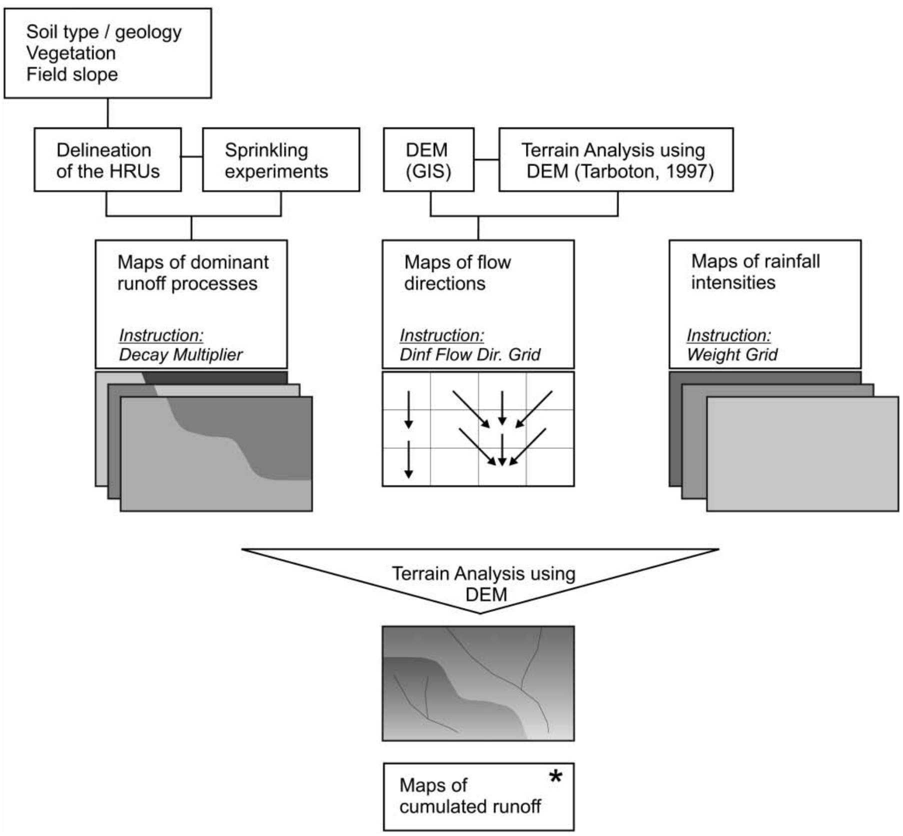

Figure 2 | Steps to realize maps of cumulated runoff in Innerrrüteni in Kandergrund; *time is not considered.

(2004), who attributed a value of RC and slope to each class; altogether, six classes were considered, which corresponded to risk of the predisposition to surface runoff, increasing from 1 to 6 (class 1 for $0 < RC < 0.1$; class 2 for $0.11 < RC < 0.30$; class 3 for $0.31 < RC < 0.50$; class 4 for $0.51 < RC < 0.75$; class 5 for $0.75 < RC$ and class 6 for $RC = 1$).

(iii) Sprinkling experiments of same intensities were carried out on the plot of 16 m^2 surface area and similar experiments repeated on six selected plots of 1 m^2 (within 16 m^2) representing two slope classes (10–15° and 15–20°) and obtained values attributed to the other plots of similar slope that are not investigated (within 16 m^2) (Figure 1(c)). To avoid the risk that the first irrigation might influence the next within the plot of 16 m^2, the time interval between the experiments was set to one day according to the following order: D1, D3, C2, B3, D2, and C2.

(iv) Flow directions were then determined on the plot of 16 m^2 surface area according to the principle of Tarboton (1997). The RC is also attributed to each flow direction of a pixel (2×2 m). Calculated RC within 16 m^2 was compared against measured surface runoff at this scale.

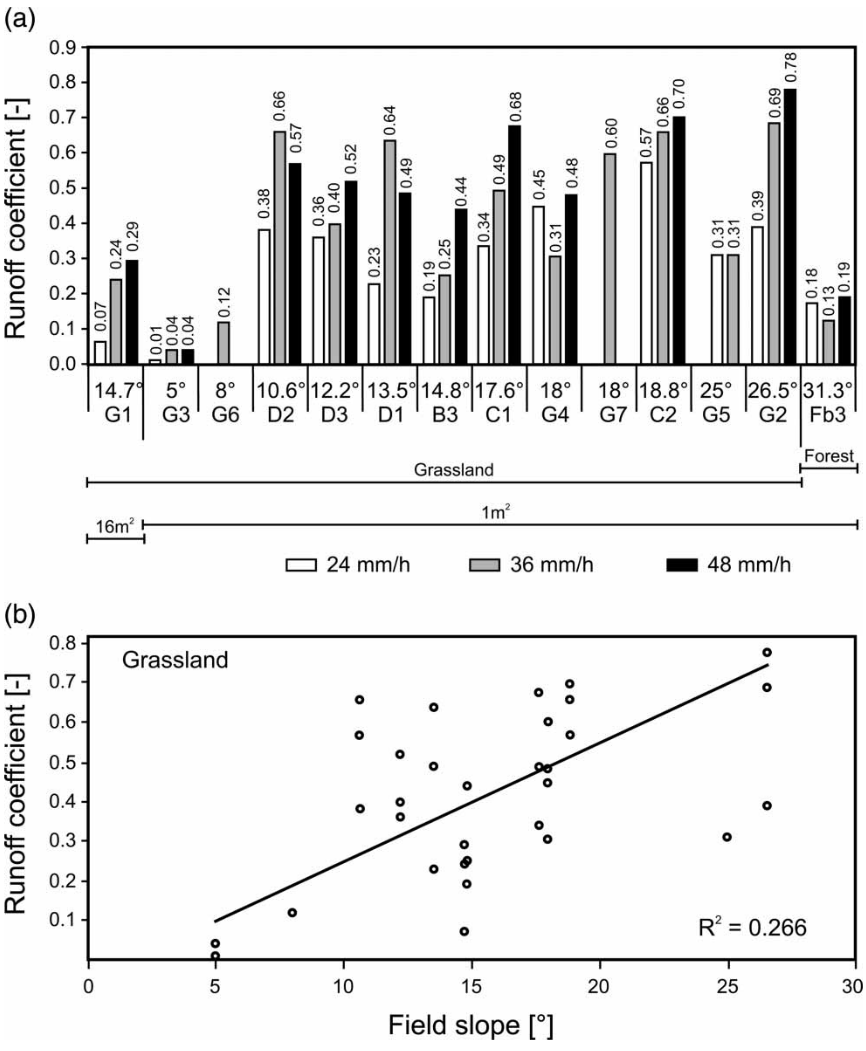

Figure 3 | Measured runoff coefficients for all investigated plots (in a) and runoff coefficient v. slope (in b).

(v) For up-scaling runoff at the catchment scale under consideration, the above steps were applied using ArcGIS 9.3 and the program TauDEM (Figure 2).

Terrain analysis using digital elevation model (TauDEM)

Flow directions based on DEMs are needed in hydrology to determine the paths of water, sediment and contaminant movement. The motivation for choosing the DEM defined by Tarboton (1997) is justified by the following factors:

(i) the need to avoid or minimize dispersion;
(ii) the need to avoid grid bias, due to the orientation of the numerical grid;
(iii) the precision with which flow directions are resolved;
(iv) a simple and efficient grid-based matrix storage structure.

Many of the functions in TauDEM are based on the D-infinity ($D\infty$) multiple flow direction model (Tarboton 1997) which represents flow direction as a vector along the direction of steepest slope on eight triangular facets centred at each grid cell. The use of triangular facets avoids the approximation involved in fitting a plane and the influence of higher neighbours on downslope flow. Where the direction does not follow one of the cardinal (0, $\pi/2$, π, $3\pi/2$) or diagonal ($\pi/4$, $3\pi/4$, $5\pi/4$, $7\pi/4$) directions, upslope area is calculated by apportioning the flow from a pixel between the two downslope pixels, according to how close the flow angle is to the direct angle to that pixel centre. As only a single number needs to be saved for each pixel to represent the flow field, computer storage is simple and efficient.

A block-centred representation is used with each elevation value taken to represent the elevation of the centre of the corresponding pixel. Eight planar triangular facets are formed between the pixel and its eight neighbours. Each of these has a downslope vector which when drawn outwards from the centre may be at an angle that lies within or outside the 45° ($\pi/4$ radian) angle range of the facet at the centre point. If the slope vector angle is within the facet angle, it represents the steepest flow direction on that facet. If the slope vector angle is outside a facet, the steepest flow direction associated with that facet is taken along the steepest edge. The flow direction associated with the pixel is taken as the direction of the steepest downslope vector from all eight facets.

RESULTS

Runoff processes

In this study, the runoff process is discussed on the basis of soil moisture and RC measurements. Change in volumetric soil moisture content (θ) in response to irrigation was analysed with reference to the initial and maximum soil moisture values, θ_{init} and θ_{max}. Thus, $\Delta\theta$ defined as the difference between θ_{max} and θ_{init} shows the magnitude of the

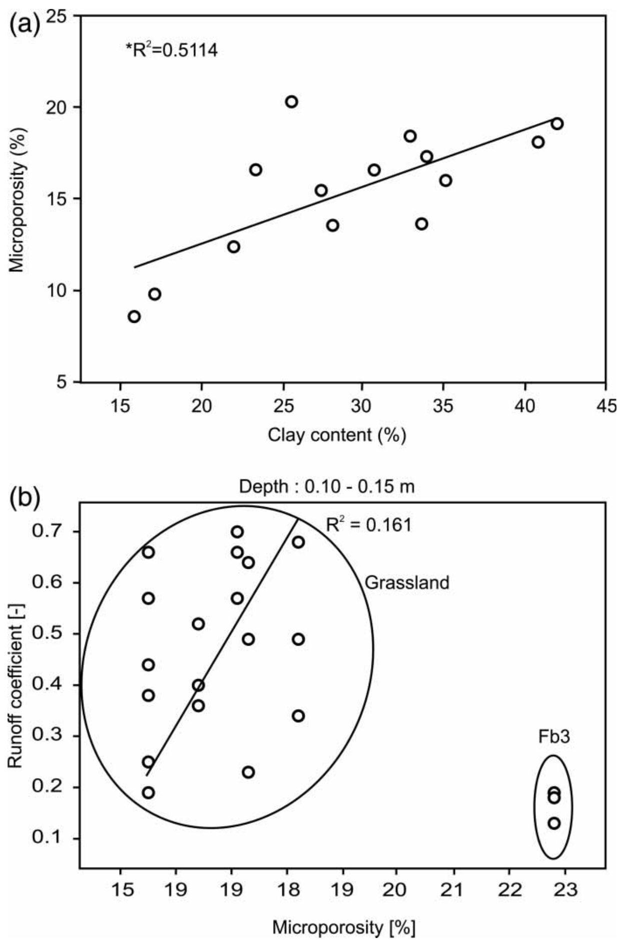

Figure 4 | Micropore volume vs. clay content (in a) and runoff coefficient versus microporosity for the three irrigation intensities of 24, 36 and 48 mm h^{-1} (in b) (The analyses of the texture and PSD were not defined on same samples and soil depths resulting in different number of measurements).

increase of soil moisture, and Δsat ($=n - \theta_{max}$) obtained from the difference between the porosity, n and θ_{max} measured during infiltration, is defined as the storage capacity of soil layer under consideration.

Surface runoff was observed at the soil surfaces of all grassland plots (Figure 3(a)) and of only a single forest plot, Fb3, with RC of 0.18, 0.13 and 0.19 for irrigation intensities of 24, 36 and 48 mm h^{-1}, respectively. In comparison, the values of RC for grassland were variable. For example, they were equal to 0.38, 0.66 and 0.57 for D2 (10.6°), and 0.19, 0.25 and 0.44 for G2 (26.5°) for irrigation intensities of 24, 36 and 48 mm h^{-1}, respectively, and 0.38 for G3 (5.0°) for the intermediate irrigation intensity of 36 mm h^{-1}. While the forest soil with the steepest slope (Figure 3(a)) produced some runoff, the grassland plot (B3) with the steepest slope (14.8°) had a lower runoff than D2 (10.6°), which generates higher RC.

As confirmed in several studies, field slope is a key parameter influencing runoff generation (e.g., Markart *et al.* 1997; Scherrer & Naef 2003). Accordingly, the correlation between these parameters measured in the areas under consideration is analysed. Figure 3(b) (illustrating RC versus slope) shows that field slope alone does not control runoff generation ($r^2 = 0.266$, p value $= 0.001813$).

Two interesting questions arise out of the obtained results and will be discussed below: (i) why did only forest soil Fb3 with the steepest slope generate surface runoff, and (ii) what caused the high RC values in the grassland soil with the gentlest slopes?

Examination of the soil textural structure of all plots, reveals that the clay content is higher in the topsoil layers of the plots that generate surface runoff (Fb3, B3, G1/G2, G3 and G4) than in the topsoil layers of the plots without surface runoff (Fa1, Fa2, Fa3, Fb1 and Fb2) (Table 2). On the one hand, it appears that clay content is linearly correlated with microporosity (Figure 4) and on the other hand, a tendency for a positive correlation between microporosity and RC exists. One possible explanation is that microporosity in grassland topsoil down to 0.35 m promotes matrix flow and delays water routing into macropores. Additional analysis in the topsoil layer between 0 and 0.10 m is needed to confirm this.

Examination of the storage capacity (Δsat) shows that the values obtained for forest soil are significantly higher than those for grassland soil (Figure 5). Any influence of external weather factors can be ruled out because the infiltration experiments were carried out during the same periods in the summer season, excluding any precipitation events during at least one week. The higher storage capacity of forest soil is probably due, on the one hand, to more intense root water uptake capacity by trees (Figure 6), and on the other, by the larger unsaturated hydraulic conductivity of forest soil. In fact, Figure 6 exhibits significantly higher

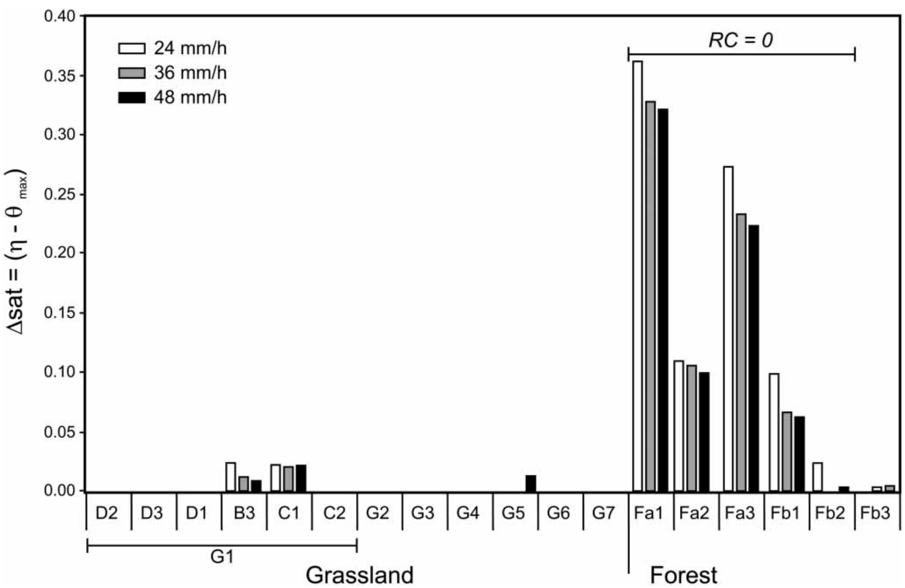

Figure 5 | Storage capacity (Δsat) in grassland and forest soils, defined as the difference between total porosity and maximal soil moisture measured during infiltration.

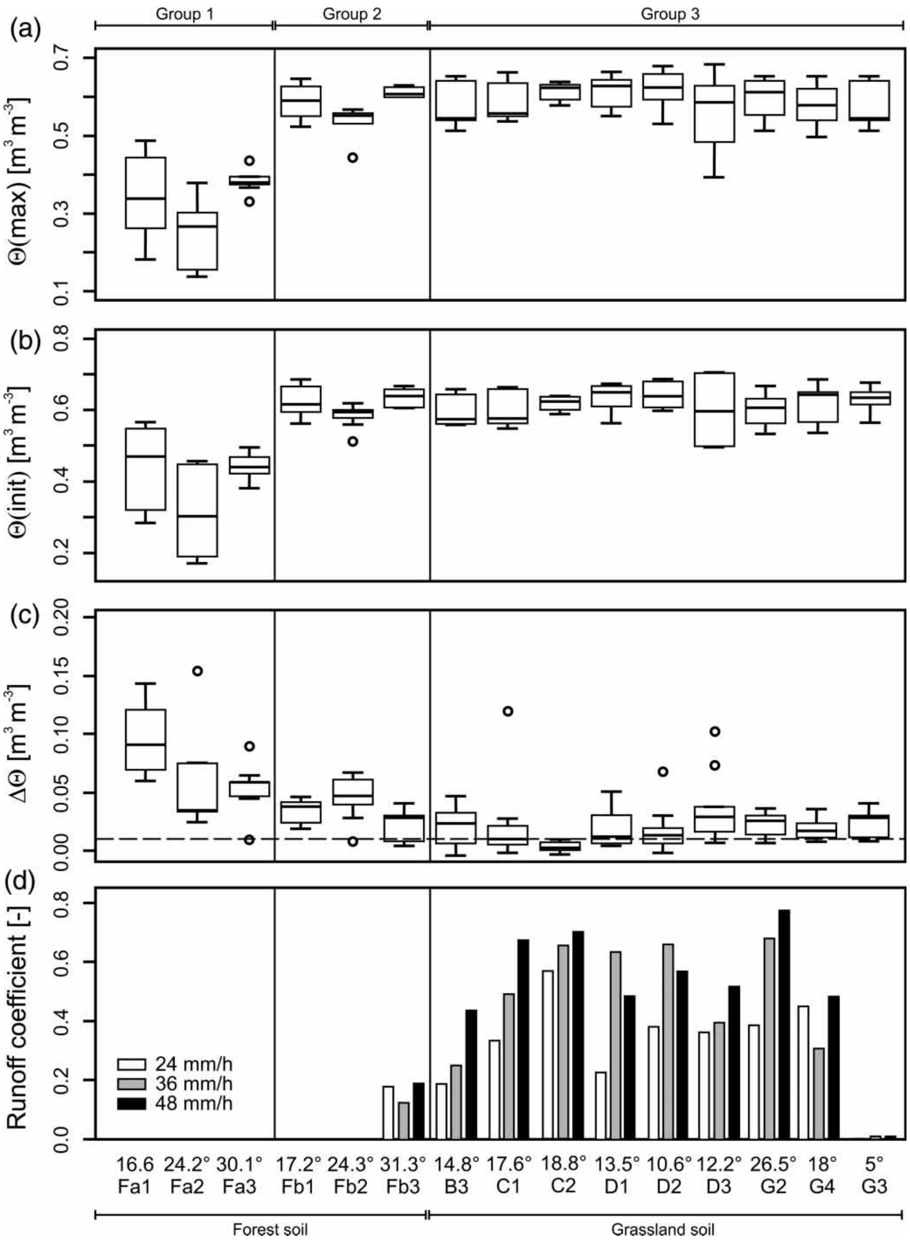

Figure 6 | Analysis of soil moisture variation (a, b and c) and runoff coefficient (d) in the forest and grassland soil. The groups of plots were compared two by two: 1–2, 1–3* and 2–3 with a significance of 95%. Each box contains 9 measurements (three irrigation intensities and three (topsoil) depths); plots G1, G5, G6 and G7 are not considered because of insufficient data (*only groups 1 and 3 are significantly different for θ_{max}, θ_{init} and $\Delta\theta$).

values of $\Delta\theta$ especially in forest soil Fa (Group 1) compared with grassland soil (Group 3). Similarly, Badoux *et al.* (2006) reported that sprinkling experiments on dry to humid Cambisols in forested catchments result in no or only low RC values varying between 0.01 and 0.16. They showed that RC was considerably higher after dry antecedent conditions than after wet antecedent conditions, which is probably due to water repellence. In contrast, artificial high intensity precipitation on plots of 1 m^2 plots in forest soil leads to high RC values (from 0.39 to 0.94) on humid to wet gleysols (Badoux *et al.* 2006). These results are rather unexpected for forest soils, which often do not generate any surface runoff at all (e.g., Schwarz 1986; Kohl *et al.* 1997; Markart *et al.* 1997). The fact that surface runoff was found only in

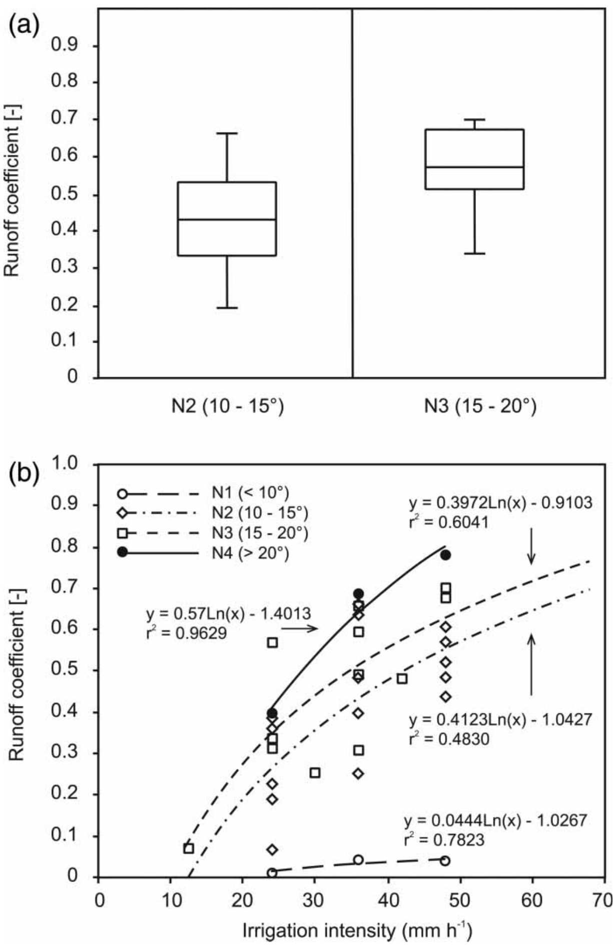

Figure 7 | Measured runoff coefficient for different field slopes; (a) significant difference between runoff coefficient of the two main slope classes N2 (10–25°) and N3 (15–20°), and (b) measured runoff coefficient versus irrigation intensities for all field slopes.

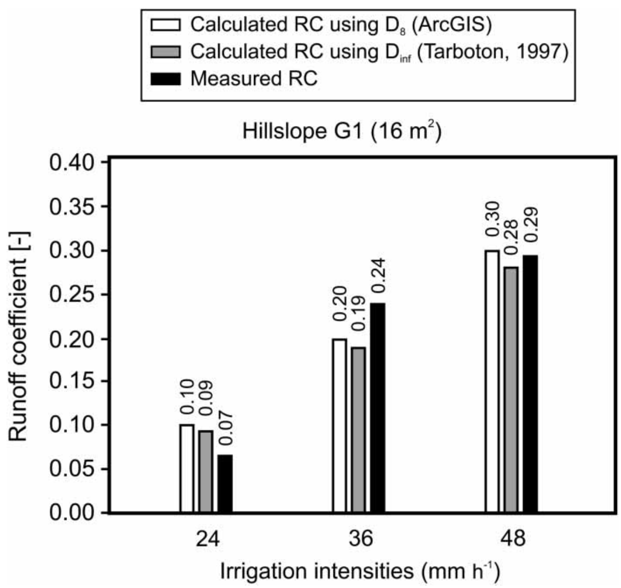

Figure 8 | Calculated runoff coefficients (D8 and D_{inf}) in grassland soil G1 (16 m^2) v. measured ones.

Fb3 compared with Fb1 and Fb2 can be explained as follows:

(i) Fb3 has the steepest slope (31.3°) compared with slopes in the other forest plots;
(ii) Fb3 has the highest clay content in comparison with the two other plots Fb1 and Fb2 (37.6% in Fb3 against 26.5% in Fb1 and 21.3% in Fb2 according to the mean values throughout entire soil profiles, and 28.1% in Fb3 against 17.1% in Fb1 and 15.7% in Fb2 when considering topsoil up to 0.15 m depth) (Table 2).

In view of these results, it appears that the two types of vegetation have distinct effects on soil structure leading to two major flow processes, vertical infiltration in forest soil and surface runoff in grassland soil. These observations are only partially in agreement with the literature and cannot be extrapolated to the wide range of soils in other regions in Switzerland. Scherrer (1996) carried out irrigation experiments on grassland and arable land in Switzerland in regions with soils of different geological origin. High variability in runoff generation that depended on the local situation was shown, mainly depending on soil properties and geology. Using irrigation experiments, Weiler *et al.* (1998) reported that runoff generation on grassland was mainly controlled by a highly permeable A horizon; the vertical macropore system in deeper layers controlled bypass flow. In contrast, the same authors (Weiler *et al.* 1998) found a stronger subsurface flow response for forest soils with a bimodal pore size distribution. Markart *et al.* (1997) reported favourable conditions in the forest regarding fast runoff mitigation.

Up-scaling of runoff processes

Results of runoff measurements show that water flows laterally at the soil surface on all plots with grassland soils. Two main slope classes N2 and N3 (10–15° and 15–20°, respectively) are statistically distinguished in relation to the RC values obtained in grassland soils (Figure 7(a)). Additional plots with different slopes (N1<10° and N4>20°) were

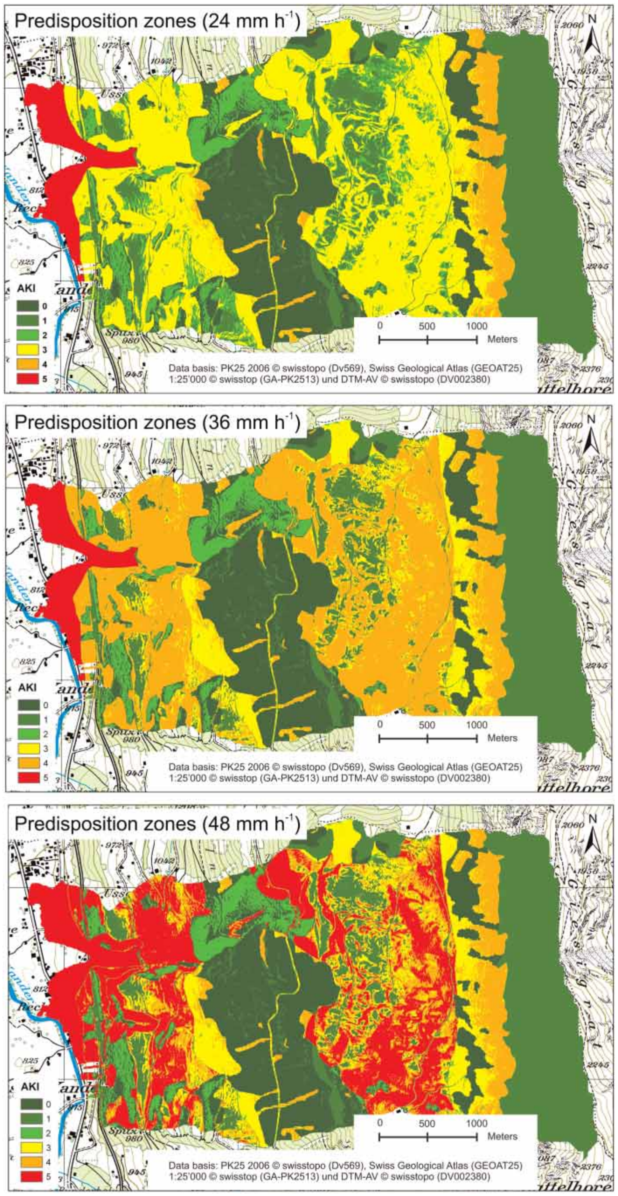

Figure 9 | Maps of the predisposition zones (according to Markart *et al*. 2004) in the Kandergrund valley, produced with sprinkling experiments and delineation of hydrological response units (HRUs), defined from the soil data, geology, topography and vegetation.

summarily investigated to improve the accuracy of the prediction at large scale (Figure 7(b)). Although there are only three investigated plots per slope class, they clearly indicate distinct behaviour in comparison with the other two.

When considering the 16 m^2 plot, a good correlation was observed between measured RC and calculated RC using D_{inf} according to Tarboton (1997) especially during low and high irrigation intensities (Figure 8). Calculated RC according to D8 (simple extrapolation considering the eight neighbouring pixels) is better correlated with measured RC during the intermediate irrigation intensity (36 mm h^{-1}) but the difference is negligible when compared with RC calculated using D_{inf}.

The maps of the zones with predisposition to surface runoff classified according to Markart *et al.* (2004) show areas in the low predisposition classes located principally in the eastern and central parts of the catchment under consideration, corresponding to limestone outcrop and forest soils, respectively (Figure 9). In addition, it appears that increasing the irrigation intensity from 24 to 48 mm h^{-1} increases the risk of the predisposition to surface runoff from 3 to 5, respectively, in the major parts of the catchment on both sides of the forest. Additional insights can be drawn from these maps: grassland areas are more subject to surface runoff with variable values, depending especially on field slopes. In contrast, forest soils generate vertical percolation in all cases except on the plot of a slope greater than 31.3°.

The maps of the flow directions obtained using the TauDEM (Tarboton 1997) shown in Figure 10 highlight two main observations:

(i) Surface runoff converges in the channels which constitute the main lateral flow pathways and the cumulated runoff increases, generally in the direction of flow (Table 3);
(ii) Two main areas composing the catchment under consideration are distinguished: A (2.3 km^2) and B (1.5 km^2) which contain two independent flow networks resulting in final outlets O-A7 and O-B6, respectively (Figure 10).

For a rainfall intensity of 48 mm h^{-1}, estimated volume was 40,270 m^3 in O-A7 and 18,030 m^3 in O-B6, showing the great difference between the sub-catchments. This is also the case for the RC which is twice as high in A as in B. Increasing rainfall intensity, from 24 to 36 mm h^{-1}, increases the risk of the predisposition to surface runoff from weak to medium when considering the entire catchment (Figure 11).

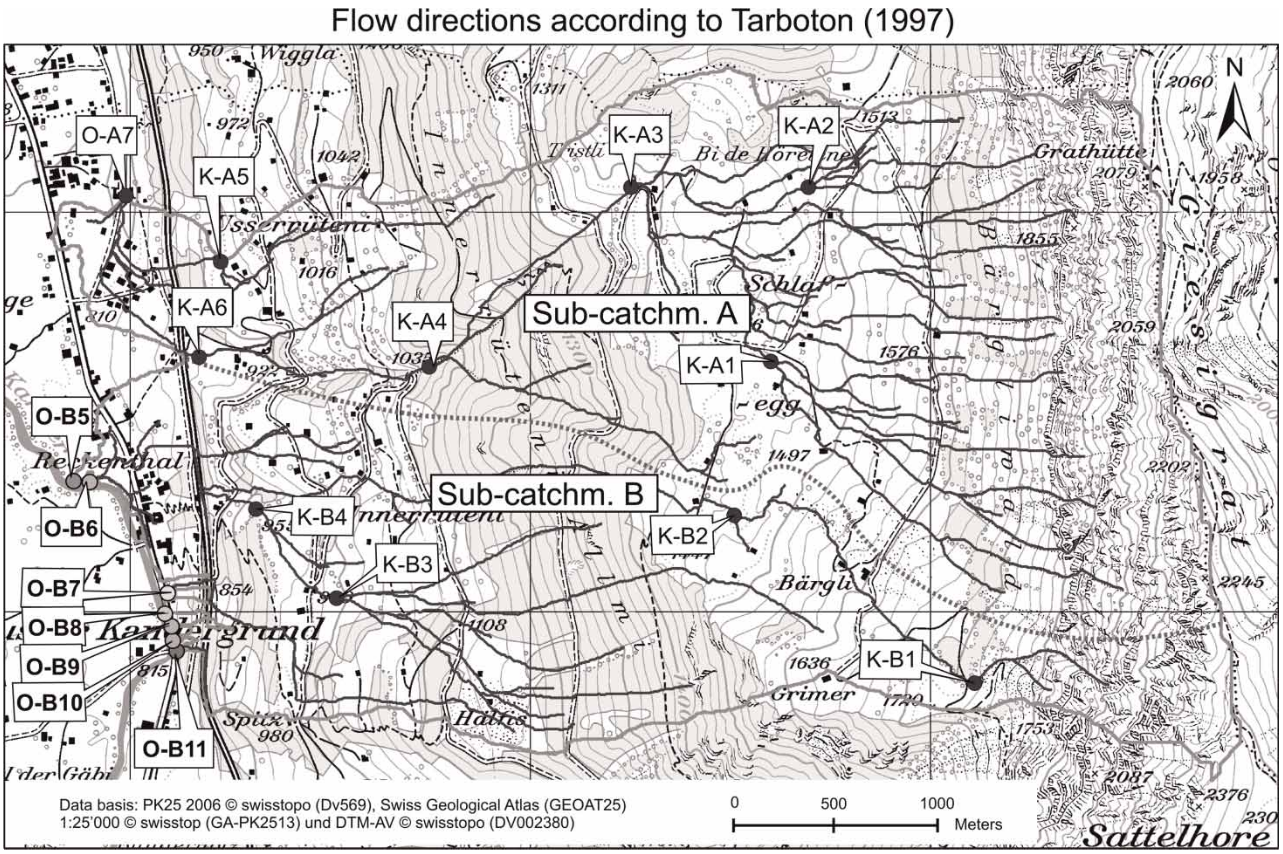

Figure 10 | Map of the flow network defined by the terrain analysis using digital elevation model according to Tarboton (1997).

When considering the change in RC in space scale, it appears that in the sub-catchment A, calculated runoff increased continually from 300 m^3 (in KA2) to 4,944 m^3 (KA4) and decreased to 3,380 m^3 in KA6 because of the forest soil of the predisposition class 1 that infiltrates a considerable portion of the water (Figure 10 and Table 3). By contrast, in the sub-catchment B the volume of water increased from 321 m^3 in KB1 to 1,698 m^3 in KB2, and decreased to 1,118 m^3 in KB4 due to the high infiltration capacity of the forest soil (predisposition class 1). The considerable increase in the water volume from KA2 to KA4 can be explained, in addition to the change in the zones of predisposition from 1 to 3, by the existence of the high number of channels that help to supply the target outlet KA4, in comparison with what happened in the sub-catchment B. Taking these results into account, two observations can be made:

(i) It seems that not only the spatial sequence of zones with predisposition to surface runoff plays an important role, but also the tortuosity and length of channels, which enhance the cumulated volume reaching the target outlets;
(ii) The TauDEM-based method is a useful tool to complete the information given by the maps of the predisposition zones, which fail to give information on the change in the processes in space scale.

When using an independent method such as the one described by Rickli & Forster (1997), which relies on the assumption of hydrologically homogeneous sub-catchments allowing for an objective and replicable evaluation of RC, the RC values obtained were between 0.45 and 0.50 for the same catchment (Zgraggen 2009). Although these results are slightly higher than those obtained using TauDEM ($RC = 0.34$ for a rainfall intensity of 48 mm h^{-1}), they confirm the estimations made in this study. The estimation error of the Rickli and Forster method was evaluated to be ±20% (Dobmann 2009). The difference between the results obtained can be explained by the fact that the method

Table 3 | Calculated water volumes and runoff coefficients in the catchment under consideration according to Tarboton (1997)

Outlet	Volume [m³]			Runoff coefficient [–]		
See fig.	24 mm/h	36 mm/h	48 mm/h	24 mm/h	36 mm/h	48 mm/h
KA1	3,070	5,543	7,890	0.0338	0.0407	0.0434
KA2	300	577	841	0.0033	0.0042	0.0046
KA3	3,906	7,490	10,746	0.0430	0.0550	0.0592
KA4	4,944	9,621	13,972	0.0545	0.0706	0.0769
KA5	1,108	2,486	3,924	0.0122	0.0183	0.0216
KA6	3,379	6,606	9,674	0.0372	0.0485	0.0533
O-A7 (A)	14,083	27,358	40,273	0.16	0.20	0.22
KB1	321	474	653	0.0035	0.0035	0.0036
KB2	1,698	3,580	5,521	0.0187	0.0263	0.0304
KB3	1,038	1,844	2,785	0.0114	0.0135	0.0153
KB4	1,018	2,160	3,263	0.0112	0.0159	0.0180
O-B5	24	36	48	0.0003	0.0003	0.0003
O-B6	6,027	11,993	18,029	0.0664	0.0881	0.0993
O-B7	1,121	2,371	3,554	0.0123	0.0174	0.0196
O-B8	61	119	182	0.0007	0.0009	0.0010
O-B9	10	19	29	0.0001	0.0001	0.0002
O-B10	11	21	31	0.0001	0.0002	0.0002
O-B11	90	196	309	0.0010	0.0014	0.0017
Subcatchm. B	7,344	14,755	22,182	0.08	0.11	0.12
Whole catchm.	21,427	42,113	62,455	0.24	0.31	0.34

used in this study is based on local hydrodynamic response, whereas the Rickli and Forster method infers the hydrologic reaction from soil properties and land use, with the aim of delineating the locations of different reactions to precipitation within the catchment.

Although the TauDEM-based method gave satisfactory results in terms of flow processes, additional consideration of the geology is needed to take the deep flow percolation into account for the runoff calculations. Further *in-situ* measurements of runoff under natural events at different outlets in a gauged catchment are needed to validate the estimated values and to take into account the changes in runoff processes on a temporal scale.

CONCLUSIONS

The main aims of this study were: (i) to identify and characterize flow processes at the plot scale, and (ii) to up-scale this knowledge to the catchment scale, by combining maps showing flow directions, with maps of zones with a predisposition to surface runoff and *in-situ* sprinkling experiments.

The marked differences in the textural and structural porosities between forest and grassland plots appear to control runoff processes. On the one hand, forest soil has a higher storage capacity than grassland soil, probably caused by large unsaturated hydraulic conductivity and root water uptake resulting in lower surface runoff. On the other hand, fine material present in the topmost ten centimetres helps to generate a structure that is probably unfavourable to vertically downward percolation and thus enhances surface runoff as observed on the grassland plots. However, within each soil category, slope plays an important role in generating surface runoff.

The method based on the Terrain Analysis Using Digital Elevation Model (TauDEM) (Tarboton 1997) was calibrated on 16 m^2 plot. Validation at this scale gave

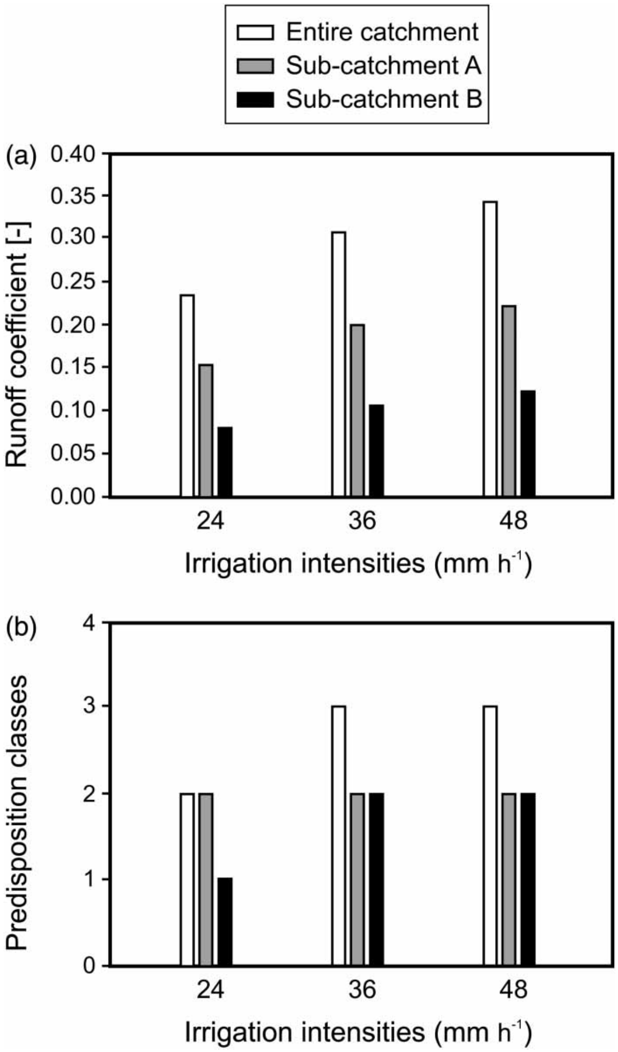

Figure 11 | (a) Calculated runoff coefficients in the entire catchment and sub-catchments A and B, and (b) evolution of the predisposition classes with intensities.

satisfactory results in terms of surface runoff. In total, 57 sprinkling experiments carried out on grassland and forest soils with three different irrigation intensities were used to up-scale surface runoff in the small catchment under consideration.

Up-scaling runoff processes using TauDEM based on sprinkling experiments gave more quantitative insight into flow processes such as flow directions and runoff quantification and traced the hydrological connectivity between the zones of predisposition. Moreover, *in-situ* investigations are needed in order to validate the runoff estimation at the catchment scale.

ACKNOWLEDGEMENTS

The authors wish to thank Bernhard Wehren and Judith Dobmann for providing us with useful information on the investigated catchment.

REFERENCES

Alaoui, A. & Helbling, A. 2006 Evaluation of soil compaction using hydrodynamic water content variation: comparison between compacted and non-compacted soil. *Geoderma* **134**, 97–108.

Alaoui, A., Germann, P., Jarvis, N. & Acutis, M. 2003 Dual-porosity and kinematic wave approaches to assess the degree of preferential flow in an unsaturated soil. *Hydrol. Sci. J.* **48**, 455–472.

Anderson, M. G. & Burt, P. 1990 *Process Studies in Hillslope Hydrology*. John Wiley & Sons Ltd., Chichester, UK, 539 pp.

Badoux, A., Witzig, J., Germann, P., Kienholz, H., Lüscher, P., Weingartner, R. & Hegg, C. 2006 Investigations on the runoff generation at the profile and plot scales, Swiss Emmental. *Hydrol. Proc.* **20**, 377–394.

Beven, K. 1995 Linking parameters across scales: subgrid parameterizations and scale dependent hydrological models. *Hydrol. Proc.* **9**, 507–525.

Beven, K. & Kirkby, M. J. 1979 A physically based variable contributing area model of basin hydrology. *Hydrol. Sci. Bull.* **24**, 43–69.

Beven, K., Kirkby, M. J., Schofield, N. & Tagg, A. F. 1984 Testing a physically based flood forecasting model (TOPMODEL) for three UK catchments. *J. Hydrol.* **69**, 119–143.

Boorman, D. B., Hollis, J. M. & Lilly, A. 1995 Hydrology of soil types: a hydrologically-based classification of the soils of the United Kingdom. Institute of Hydrology, Report no. 126.

Buttle, J. M. & McDonald, D. J. 2002 Coupled vertical and lateral preferential flow on a forest slope. *Water Resour. Res.* **38** (5), 17.

Dobmann, J. 2009 Hochwasserabschätzung in kleinen Einzugsgebieten der Schweiz [Flood Estimation in Small Swiss Catchments]. Interpretations-und Praxishilfe. Dissertation. Geographisches Institut der Universität Bern, Schweiz, 301pp.

Fiès, J. C. 1992 Analysis of soil textural porosity relative to skeleton particle size, using mercury porosimetry. *Soil Sci. Soc. Am. J.* **56**, 1062–1067.

Furrer, H., Huber, K., Adrian, H., Baud, A., Flück, W., Preiswerk, C., Schuler, P., Zwahlen, P., Ackermann, A., Arnold, P., Ferrazzini, B. & Genge, E. 1993 Geologischer Atlas der Schweiz, 1:25′000, Adelboden (LK 1247), Blatt 87 [Swiss Geological Atlas, 1:25,000, Adelboden (LK 1247), Sheet no. 87]. Landshydrologie und-Geologie, Bern, Switzerland.

Kohl, B., Markart, G., Stary, U., Proske, H. & Trinkaus, P. 1997 Abfluss-und Infiltrationsverhalten von Böden unter Fichtenalbeständen in der Gleinalm (Stmk.) [Drainage and infiltration characteristics of spruce forest soils in the

'Gleinalm' alp (Steiermark)]. *Berichte der Forstlichen Bundesversuchsanstalt Wien* **96**, 27–32.

Konen, M. E., Jacobs, P. M., Lee Burras, C., Talaga, B. J. & Mason, J. A. 2002 Equations for predicting soil organic carbon using loss-on-ignition for North Central U.S. Soils. *Soil Sci. Soc. Am. J.* **66**, 1878–1881.

Luxmoore, R. J. 1981 Micro-, meso- and macroporosity of soil. *Soil Sci. Soc. Am. J.* **45**, 671–672.

Maréchal, D. & Holman, I. P. 2004 Comparison of Hydrologic Simulations Using Regionalised and Catchment-Calibrated Parameter Sets for Three Catchments in England. Transactions of the 2nd Biennial Meeting of the International Environmental Modelling and Software Society, IEMSs, Manno, Switzerland, 2004, 145 pp.

Markart, G., Kohl, B. & Zanetti, P. 1997 Oberflächenabfluss bei Starkregen – Abflussbildung auf Wald-, Weideund Feuchtflächen (am Beispiel des oberen Einzugsgebietes der Schesa – Bürserberg, Vorarlberg) [Surface runoff during storms – runoff formation from forested and wetland areas (using the example of the upper catchment area of the Schesa – Bürserberg, Vorarlberg)]. *Centralblatt für das gesamte Forstwesen* **114**, 123–144.

Markart, G., Kohl, B., Sotier, B., Schauer, T., Bunza, G. & Stern, R. 2004 Provisorische Geländeanleitung zur Abschätzung des Oberflächenabflussbeiwertes auf alpinen Boden-/Vegetationseinheiten bei konvektiven Starkregen [A simple Code of Practice for Assessment of Surface Runoff Coefficients for Alpine Soil-/Vegetation Units in Torrential Rain] (Version 1.0). BFW Dokumentationen. Bundesamt und Forschungszentrum für Wald, Wien.

McDonnell, J. J. 2003 Where does water go when it rains? Moving beyond the variable source area concept of rainfall–runoff response. *Hydrol. Proc.* **17**, 1869–1875.

Moore, I. D., Grayson, R. B. & Ladson, A. R. 1991 Digital terrain modelling: a review of hydrological, geomorphological, and biological applications. *Hydrol. Proc.* **5**, 3–30.

Peschke, G., Etzenberg, C., Müller, G., Töpfer, J. & Zimmermann, S. 1999 Die Abflussbildung in ihrer Abhängigkeit von der wirksamen Kombination flächenvariabler Einflussfaktoren und Gebietszustand [Runoff generation depending of the effective combination of spatial variable factors and antecedent conditions]. Abschlussbericht zur Forschung, DFG-Schwerpunkt Programm 'Regionalisierung in der Hydrologie'. Internationales Hochschulinstitut Zittau, Zittau, Germany.

Rickli, C. & Forster, F. 1997 Einfluss verschiedener Standorteigenschaften auf die Schätzung von Hochwasserabflüssen in kleinen Einzugsgebieten [Impact of different site properties on the estimation of the flood discharges in small catchments]. *Schweizerische Zeitschrift für Forstwesen* **148**, 367–385.

Roth, K., Schulin, R., Flühler, H. & Attinger, W. 1990 Calibration of time domain for reflectometry water content measurement using a composite dielectric approach. *Water Resour. Res.* **26**, 2267–2274.

Schädler, B. & Weingartner, R. 1992 Natürliche Abflüsse 1961–1980 [Natural discharge 1961–1980]. In: *Hydrologischer Atlas der Schweiz, Tafel 5.4*. Bundesamt für Landestopographie, Wabern, Switzerland.

Scherrer, S. 1996 Abflussbildung bei Starkniederschlägen–Identifikation von Abflussprozessen mittels künstlicher Niederschläge [Runoff generation during intense rainfall-identification of runoff processes using sprinkling experiments]. PhD thesis no. 11793, Swiss Federal Institut of Technology, ETH, Zurich.

Scherrer, S. & Naef, F. 2003 A decision scheme to identify dominant flow processes at the plot-scale for the evaluation of contributing areas at the catchments-scale. *Hydrol. Proc.* **17**, 391–401.

Scherrer, S., Naef, F., Fach, A. O. & Cordery, I. 2007 Formation of runoff at the hillslope scale during intense precipitation. *Hydrol. Earth Syst. Sci.* **11**, 907–922.

Schmocker-Fackel, P., Naef, F. & Scherrer, S. 2007 Identifying runoff processes on the plot and catchment scale. *Hydrol. Earth Syst. Sci.* **11**, 891–906.

Schwarz, O. 1986 Zum Abflussverhalten von Waldböden bei künstlicher Beregnung [Runoff characteristics of forest soils as affected by artificial irrigation]. In: *DFG–Research Report on the landscape ecological project 'Schönuch'* (G. Einsele, ed.), VCH Publisher, Weinheim, pp. 161–179.

Sekera, F. 1951 *Gesunder und kranker Boden [Healthy and sick soil]*. 3rd edition, Paul Parey Publisher, Berlin, 95 pp.

Soil Survey Staff 2003 *Keys to Soil Taxonomy. Soil Survey Staff, 0120*. U.S. Dept. of Agriculture, Natural Resources Conservation Service, Washington, D.C.

Soil Survey Staff 2004 Soil survey laboratory methods manual. Soil Survey Investigations Report No. 42, Version 4.0, Natural Resources Conservation Service, National Soil Survey Center, United States Department of Agriculture, Lincoln, New England.

Tarboton, D. G. 1997 A new method for the determination of flow directions and upslope areas in grid digital elevation models. *Water Resour. Res.* **33**, 309–319.

Weiler, M., Naef, F. & Leibundgut, C. 1998 Study of runoff generation on hillslopes using tracer experiments and a physically-based numerical hillslope model. In: *Hydrology, Water Resources and Ecology in Headwaters* (K. Kovar, U. Tappeiner, N. E. Peters & R. G. Craig, eds.). IAHS Publication 248, IAHS Press, Wallingford, pp. 353–360.

Wood, E. F., Sivapalan, M. & Beven, K. 1990 Similarity and scale in catchment storm response. *Rev. Geophys.* **28**, 1–18.

Zgraggen, S. 2009 Hochwasserverhältnisse in kleinen Teileinzugsgebieten der Kander [Conditions to Flood in Small Catchments of the Kander Region]. Masterarbeit, Gewässerkunde Nr. 441, Geographisches Institut der Universität Bern, Schweiz, p. 209.

First received 5 July 2010; accepted in revised form 24 March 2011. Available online 27 January 2012